AD-A035 180 STEVENS INST OF TECH HOBOKEN N J DAVIDSON LAB F/G 13/10
STEADY AND UNSTEADY LOADINGS AND HYDRODYNAMIC FORCES ON COUNTER--ETC(U)
JUL 76 S TSAKONAS, W JACOBS, M ALI N00014-67-A-0202-0047
UNCLASSIFIED SIT-DL-1899 NL

1 OF 1
ADA035180

END

DATE
FILMED
3 - 77

R-1899

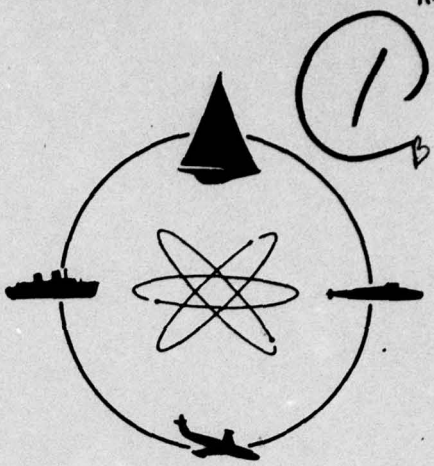

DAVIDSON LABORATORY

Report SIT-DL-76-1899

July 1976

STEADY AND UNSTEADY LOADINGS AND HYDRODYNAMIC FORCES ON COUNTERROTATING PROPELLERS

by

S. Tsakonas, W. Jacobs and M. Ali

STEVENS INSTITUTE OF TECHNOLOGY

CASTLE POINT STATION
HOBOKEN, NEW JERSEY 07030

This study has been conducted under the combined support of the Naval Sea Systems Command General Hydrodynamics Research Program under Contract N00014-67-A-0202-0047 and N00014-75-C-0483 and the Office of Naval Research under Contract N00014-76-M-0023 (NR062-549)

UNCLASSIFIED

SECURITY CLASSIFICATION OF THIS PAGE (When Data Entered)

REPORT DOCUMENTATION PAGE

READ INSTRUCTIONS BEFORE COMPLETING FORM

1. REPORT NUMBER: Report SIT-DL-76-1899
2. GOVT ACCESSION NO.
3. RECIPIENT'S CATALOG NUMBER
4. TITLE (and Subtitle): Steady and Unsteady Loadings and Hydrodynamic Forces on Counterrotating Propellers
5. TYPE OF REPORT & PERIOD COVERED: Final/1 Feb 1974 - 31 Jan 1976
6. PERFORMING ORG. REPORT NUMBER
7. AUTHOR(s): S./Tsakonas, W./Jacobs & M./Ali
8. CONTRACT OR GRANT NUMBER(s): N00014-67-A-0202-0047, N00014-75-C-0483, N00014-76-M-0023 (NR062-549)
9. PERFORMING ORGANIZATION NAME AND ADDRESS: Davidson Laboratory, Stevens Institute of Technology, Casrle Point Station, Hoboken, N. J. 07030
10. PROGRAM ELEMENT, PROJECT, TASK AREA & WORK UNIT NUMBERS: 61153N/R02301, SR 023 01 01
11. CONTROLLING OFFICE NAME AND ADDRESS: David W. Taylor Naval Ship Research and Development Center, Code 1505, Bethesda, Md 20084
12. REPORT DATE: July 1976
13. NUMBER OF PAGES: 18 (12) 220
14. MONITORING AGENCY NAME & ADDRESS (if different from Controlling Office): Office of Naval Research, 800 N. Quincy St, Arlington, Va 22217
15. SECURITY CLASS. (of this report): UNCLASSIFIED
15a. DECLASSIFICATION/DOWNGRADING SCHEDULE
16. DISTRIBUTION STATEMENT (of this Report): APPROVED FOR PUBLIC RELEASE; DISTRIBUTION UNLIMITED
17. DISTRIBUTION STATEMENT (of the abstract entered in Block 20, if different from Report)

18. SUPPLEMENTARY NOTES: Sponsored by the Naval Sea Systems Command General Hydromechanics Research Program administered by the David W. Taylor Naval Ship Research and Development Center, Code 1505, Bethesda, Md 20084 and the Office of Naval Research
19. KEY WORDS (Continue on reverse side if necessary and identify by block number): Counterrotating Propellers, Hydrodynamic Forces, Steady and Unsteady Loading, Computer Program
20. ABSTRACT (Continue on reverse side if necessary and identify by block number):

The linearized lifting surface theory has been applied to the evaluation of blade loadings and resultant hydrodynamic forces and moments (thrust, torque, bearing forces and bending moments) of counterrotating propeller systems with equal and unequal number of blades operating in uniform and nonuniform inflow fields, both units rotating with the same RPM. The mathematical model takes into account as realistically as possible the geometry of the propulsive device, the mutual interaction of both units and the three-dimensional spatially varying inflow field. A computer program has been developed adaptable to

(cont on p. 738)

DD FORM 1 JAN 73 1473 EDITION OF 1 NOV 65 IS OBSOLETE S/N 0102-LF-014-6601

104 750

SECURITY CLASSIFICATION OF THIS PAGE (When Data Entered)

6pg

(cont'd fr p1473A)

high-speed digital computers (CDC 6600 - 7600) for counterrotating propulsion systems of equal and unequal blade number in uniform inflow for comparison with experimental results if available.

A

1473B

STEVENS INSTITUTE OF TECHNOLOGY
DAVIDSON LABORATORY
CASTLE POINT STATION
HOBOKEN, NEW JERSEY

Report SIT-DL-76-1899

July 1976

STEADY AND UNSTEADY LOADINGS AND HYDRODYNAMIC FORCES ON COUNTERROTATING PROPELLERS

by

S. Tsakonas, W. Jacobs and M. Ali

This study has been conducted under the combined support
of the Naval Sea Systems Command General Hydrodynamics Research Program
under Contract N00014-67-A-0202-0047 and N00014-75-C-0483
and the Office of Naval Research
under Contract N00014-76-M-0023 (NR062-549)

STEADY AND UNSTEADY LOADINGS AND HYDRODYNAMIC FORCES ON COUNTERROTATING PROPELLERS

S. TSAKONAS, W. JACOBS and M. ALI
Stevens Institute of Technology, Hoboken, New Jersey, USA

The linearized lifting surface theory has been applied to the evaluation of blade loadings and resultant hydrodynamic forces and moments (thrust, torque, bearing forces and bending moments) of counterrotating propeller systems with equal and unequal number of blades operating in uniform and nonuniform inflow fields, both units rotating with the same RPM. The mathematical model takes into account as realistically as possible the geometry of the propulsive device, the mutual interaction of both units and the three-dimensional spatially varying inflow field. A computer program has been developed adaptable to high-speed digital computers (CDC 6600 - 7600) for counterrotating propulsion systems of equal and unequal blade number in uniform inflow for comparison with experimental results if available.

1. INTRODUCTION

The combination of two counterrotating propellers on fast ships has been shown to offer considerable improvement in propulsive efficiency when compared with a single screw [1]. Furthermore, since the total required power is divided between two propellers, this results in a reduction of blade loadings and hence the inception of cavitation is delayed. These are the main advantages of this propulsive system; its principal disadvantage lies in the mechanical complications in transmitting power through a coaxial counterrotating shaft.

The CR (counterrotating) propulsive system is also expected to have more favorable vibrational behavior. From tests of a 4-0-5 CR system (4-bladed forward and 5-bladed after propeller) in the wake of a model of a fast cargo liner [2], it appears that the ratios of amplitudes of excitation to mean thrust are comparable to those of a single screw providing the same power. However in these tests the nonuniform wake is by far the dominating cause of vibration. The effects of the interaction of both propellers are small in comparison and the higher frequency excitations cannot be determined at all accurately.

A better understanding of the mechanism of the interaction can be obtained by considering the CR system under open-water conditions (uniform inflow field) so that wake harmonics are not present to mask the interaction phenomenon.

The calculation procedure is based on the analysis of Reference 3 for the cases of CR systems of equal and unequal blade number, operating at equal or unequal RPM in uniform and nonuniform inflow fields. In that reference the true geometry of the helicoidal blades was taken into account with the exception that blade thickness was assumed negligible.

In the present paper, CR systems of equal and unequal number of blades will be considered operating at equal RPM in a uniform inflow field. The blade thickness effects will also be considered, as additional velocity perturbations on the LH (left-hand) sides of the two surface integral equations which state the kinematic conditions on both units of the CR system.

The development of this pair of surface integral equations is based on a linearized unsteady lifting surface theory as adapted to the marine propeller case. Their kernel functions are derived by means of the acceleration potential method and the surface integrals are reduced to line integrals by employing the mode approach in conjunction with the "generalized lift operator" technique [4]. Then by the collocation method the line integral equations are reduced to two simultaneous sets of algebraic equations. Finally, the solution of these is obtained by an iterative procedure, assuming at first that the effect of the after propeller on the forward propeller, except for the velocity field due to the thickness of its blades, may be neglected.

The computation procedure adapted to a high-speed digital computer (CDC-6600 or 7600) will be utilized if experimental information will be available.

NOMENCLATURE

A	subscript index of after propeller
a	$\Omega r_o/U$
F	subscript index of forward propeller
$F_{x,y,z}$	forces in axial, horizontal and vertical directions
$I^{(\bar{m})}(x)$	defined in Equation (7a)
$I_m(\nu)$	modified Bessel function of order m
i	subscript index of control point
j	subscript index of loading point
$K_m(\nu)$	modified Bessel function of order m
K_{ji}	kernel function of integral equation
$\bar{K}_{ji}, \bar{K}^!_{ji}$	modified kernels, after chordwise-integrations
$L(r)$	spanwise loading distribution, lb/ft
$L^{(\bar{n})}(\rho)$	spanwise loading components (coefficients of chordwise distribution), lb/ft
ℓ_k	integer multiple

VIII.32

$\bar{m}$	order of lift operator
m_k	index of summation
N_F, N_A	number of blades of forward and after propellers
$\bar{n}$	order of chordwise mode
n	blade index
P	perturbation pressure
$Q_{x,y,z}$	moments about x-, y- and z-axes
q_i	order of blade harmonic
r	radial coordinate of control point
r	superscript index of control point
r_{Ao}	after propeller radius
r_{Fo}	forward propeller radius
S_j	lifting surface
t	time
U	uniform velocity
u	variable of integration
$V_i(r)$	Fourier coefficients of velocity normal to the blade
$W_i(x,r,\varphi;t)$	induced velocity at control point
x, x'	longitudinal coordinate of control point
$x(x'),r,\varphi$	cylindrical coordinate system of control points
y	horizontal Cartesian coordinate
z	vertical Cartesian coordinate
β	hydrodynamic pitch angle
ϵ	distance between the two propeller planes
$\Theta(\bar{n})$	chordwise mode
θ_j	angular coordinate of loading point
θ_α	angular chordwise location of loading point
θ_{bF}, θ_{bA}	projected semichord length, in radians, of forward and after propellers
$\bar{\theta}_{jn}$	$\frac{2\pi}{N_j}(n-1)$, n=1, ... N_j
$\theta_p(r)$	geometric pitch angle
$\Lambda^{(\bar{n})}(x)$	defined in Equation (7b)
λ_k	positive integer multiple
ξ, ξ'	longitudinal coordinate of loading point
$\xi(\xi'),\rho,\theta$	cylindrical coordinate system of loading points
ρ	radial coordinate of loading point
ρ	superscript index of loading point
ρ_f	mass density of fluid
σ	angular measure of skewness
$\Phi(\bar{m})$	generalized lift operator
φ_i	angular coordinate of control point
φ_α	angular chordwise location of control point
Ω	angular velocity of propeller (absolute value)

II. LINEARIZED UNSTEADY LIFTING SURFACE THEORY

Two counterrotating propellers are operating in the flow of an ideal incompressible fluid. The propeller arrangement and the coordinate system are shown in Figure 1.

The basic relation of the interaction phenomenon is that the negative velocities induced by the propulsion system on each propeller lifting surface should be balanced by the downwash velocity distribution at that surface, thus expressing the requirement of an impermeable boundary. The kinematic boundary conditions on both lifting surfaces are expressed as two simultaneous surface integral equations:

$$W_F(x_F,r_F,\varphi_F;t) = \iint_{S_F} \Delta P_F(\xi_F,\rho_F,\theta_F;t) \cdot K_{FF}(x_F,r_F,\varphi_F;\xi_F,\rho_F,\theta_F;t)\,dS_F + \iint_{S_A} \Delta P_A(\xi_A',\rho_A,\theta_A;t) \cdot K_{AF}(x_F,r_F,\varphi_F;\xi_A',\rho_A,\theta_A;t)\,dS_A \quad (1)$$

$$W_A(x_A',r_A,\varphi_A;t) = \iint_{S_F} \Delta P_F(\xi_F,\rho_F,\theta_F;t) \cdot K_{FA}(x_A',r_A,\varphi_A;\xi_F,\rho_F,\theta_F;t)\,dS_F + \iint_{S_A} \Delta P_A(\xi_A',\rho_A,\theta_A;t) \cdot K_{AA}(x_A',r_A,\varphi_A;\xi_A',\rho_A,\theta_A;t)\,dS_A \quad (2)$$

where

$x(x'),r,\varphi$ and $\xi(\xi'),\rho,\theta$: cylindrical coordinates of control and loading points, respectively

F and A: subscripts indicating forward and after propeller

t: time, sec

S_F, S_A: forward and after propeller surfaces, ft^2

W_F, W_A: velocity distributions normal to forward and after propellers, ft/sec

$\Delta P_F, \Delta P_A$: unknown loadings; pressure jumps across the lifting surfaces, lb/ft^2, i.e., $\Delta P = P_- - P_+$ pressure difference between back (suction side) and face (pressure side)

K_{ji}: kernel function representing the induced velocity on an element i of a blade due to unit amplitude load located at each and every element j, ft/lb-sec

The second term on the RH (right-hand side) of Eq.(1) and the first term on the RH of Eq.(2) are the interaction effects. The remaining terms are the self-induced velocities by the individual propellers.

The unknown loadings and the onset velocity distributions are cyclic in nature. Then for a CR system with right-hand aft propeller and left-hand forward propeller rotating at equal RPM

$$\Delta P_F(\xi_F,\rho_F,\theta_F;t)=\mathrm{Re}\sum_{\lambda_k=0}^{\infty}\overline{\Delta P}_F^{(\lambda_k)}(\xi_F,\rho_F,\theta_F)e^{-i\lambda_k\Omega t}$$

$$\Delta P_A(\xi_A',\rho_A,\theta_A;t)=\mathrm{Re}\sum_{\lambda_k=0}^{\infty}\overline{\Delta P}_A^{(\lambda_k)}(\xi_A',\rho_A,\theta_A)e^{i\lambda_k\Omega t} \qquad (3)$$

$$W_F(x_F,r_F,\varphi_F;t)=\mathrm{Re}\sum_{q_F=0}^{\infty}\overline{W}_F^{(q_F)}(x_F,r_F,\varphi_F)e^{-iq_F\Omega t}$$

$$W_A(x_A',r_A,\varphi_A;t)=\mathrm{Re}\sum_{q_A=0}^{\infty}\overline{W}_A^{(q_A)}(x_A',r_A,\varphi_A)e^{iq_A\Omega t} \qquad (4)$$

where q_i designates the order of shaft frequency or order of harmonic of the inflow field, λ_k that of the loading distribution to be determined by the analysis, and Ω is the absolute value of the angular velocity of each propeller. (q_i and λ_k are both positive integers.) The known downwash velocities and the unknown loadings are expressed in complex conjugate form in (3) and (4), where finally the real part is taken.

The velocities W_i are caused by flow disturbances such as those due 1) to wake, 2) to incident flow angle which is the difference between the geometric pitch angle θ_p of the propeller blade and the hydrodynamic pitch angle $\beta=\tan^{-1}U/\Omega r$ where U is forward speed and r is the radial location of the corresponding helix, 3) to blade camber, 4) to "non-planar" blade thickness, and 5) to the effects of the thickness of the blades of each propeller on the velocity field of the other. Within the limits of the linear theory, the effects of the flow disturbances can be obtained separately and then simply added together.

Although the analysis applies to both non-uniform and uniform inflow, as mentioned earlier, the solution by an iterative procedure will be restricted to the uniform inflow case (no wake). Furthermore, the disturbance due to the so-called "non-planar" thickness (since a propeller blade lies on a helicoidal surface of variable pitch, its thickness affects its own velocity field) will be ignored as negligibly small [5].

After the chordwise integrations are performed by means of the mode approach and the generalized lift operator technique, the pair of surface integral equations (1) and (2) are reduced to the following set of line integral equations for given q_i, order of shaft frequency, given $\bar{m}$, order of lift operator, and $\bar{n}$, order of chordwise mode shapes, for the case of equal RPM:

$$\frac{\bar{w}_F^{(q_F,\bar{m})}}{U}(r_F)=\int_{\rho_F}L_F^{(q_F,\bar{n})}(\rho_F)\sum_{m_1=-\infty}^{\infty}\bar{K}_{FF}^{(\bar{m},\bar{n})}(m_1=q_F+\ell_1N_F)\,d\rho_F$$
$$+\int_{\rho_F}\sum_{\lambda_2=0}^{\infty}\sum_{m_2=0}^{\infty}L_A^{(\lambda_2=q_F-2\ell_2N_A,\bar{n})}(\rho_A)\cdot\bar{K}_{AF}^{(\bar{m},\bar{n})}(m_2=q_F-\ell_2N_A)\,d\rho_A \qquad (5)$$

$$\frac{\bar{w}_A^{(q_A,\bar{m})}}{U}(r_A)=\int_{\rho_F}\sum_{\lambda_3=0}^{\infty}\sum_{m_3=0}^{\infty}L_F^{(\lambda_3=q_A+2\ell_3N_F,\bar{n})}(\rho_F)\cdot\bar{K}_{FA}^{(\bar{m},\bar{n})}(m_3=q_A+\ell_3N_F)\,d\rho_F$$
$$+\int_{\rho_A}L_A^{(q_A,\bar{n})}(\rho_A)\sum_{m_4=-\infty}^{\infty}\bar{K}_{AA}^{(\bar{m},\bar{n})}(m_4=q_A+\ell_4N_A)\,d\rho_A \qquad (6)$$

Here $L_F^{(\bar{n})}(\rho_F)$ and $L_A^{(\bar{n})}(\rho_A)$ are the unknown normal loading components of the $\bar{n}$ chordwise mode for each blade in lb/ft of span, N_F and N_A are the blade number of forward and after propellers, and ℓ_k is integer. The bars and superscripts $\bar{m}$ and $\bar{n}$ indicate that the quantities have been integrated along the chord.

The values of λ_k and m_k shown in (5) and (6) are arrived at by equating the time-dependence on LH and RH sides so that

$e^{-iq_F\Omega t}=e^{-i\lambda_1\Omega t}$ for the first term of the first integral equation

$e^{-iq_F\Omega t}=e^{i(\lambda_2-2m_2)\Omega t}$ for the second term of that equation

$e^{iq_A\Omega t}=e^{-i(\lambda_3-2m_3)\Omega t}$ for the first term of the second integral equation

$e^{iq_A\Omega t}=e^{i\lambda_4\Omega t}$ for the second term of that equation

and from the summation over all blades of a propeller which is represented by

$$\sum_{n=1}^{N}e^{\pm i(m_k-\lambda_k)\bar{\theta}_n}=\begin{cases}N & \text{for } m_k-\lambda_k=\ell_kN,\ \ell_k=0,\pm1,\ \ldots\\ 0 & \text{otherwise}\end{cases}$$

where $\bar{\theta}_n=2\pi(n-1)/N$

The respective kernels are derived in Reference 3 for RH forward propeller and LH after propeller. For LH forward and RH after propeller, they are given in the following section in final form.

III. THE KERNEL FUNCTIONS

The Kernels $\bar{K}_{FF}$ and $\bar{K}_{AA}$

These functions describe the self-induced velocity at a point on a propeller blade due to unit amplitude load at various locations on all the blades of the same propeller. The development for a right-hand propeller is given in Reference 6 and yields

$$\sum_{m=-\infty}^{\infty}\bar{K}^{(m,n)}(m=q+\ell N)=\left\{\frac{-N}{4\pi\rho_fU^2r_o}\right\}\frac{r\,e^{-iq\Delta\sigma}}{a\sqrt{1+a^2r^2}}$$
$$\sum_{m=-\infty\,m=q+\ell N}^{\infty}\left\{g(0)-\frac{i}{\pi}\int_0^{\infty}\frac{g(u)-g(-u)}{u}\,du\right\} \qquad (7)$$

where

$$g(u)=(IK)_mB'(u)e^{i\frac{u}{a}\Delta\sigma}$$

$$(IK)_m=\begin{cases}I_m(Iu+a\ell NI\rho)K_m(Iu+a\ell NIr) & \text{for } \rho<r\\ I_m(Iu+a\ell NIr)K_m(Iu+a\ell NI\rho) & \text{for } r<\rho\end{cases}$$

$$B'(u)=\left(au+a^2\ell N+\frac{m}{\rho^2}\right)\cdot\left(au+a^2\ell N+\frac{m}{\rho^2}\right)I^{(\bar{m})}\left(\left(q-\frac{u}{a}\right)\theta_b^r\right)\Lambda^{(\bar{n})}\left(\left(q-\frac{u}{a}\right)\theta_b^\rho\right)$$

ρ_f = fluid mass density, slugs/ft^3

r_o = propeller radius, ft

$\Delta\sigma=\sigma^r-\sigma^\rho$ = difference between skewness of the blade at the control point r and skewness at a loading point ρ, radians

$a=\Omega r_o/U$ and ρ and r are also non-dimensionalized by r_o

$\theta_b^r, \theta_b^\rho$ = subtended angle of projected semichord of blade at r, at ρ, radians

$I_m(\ )$ = modified Bessel function of first kind

$K_m(\ )$ = modified Bessel function of second kind

$\ell = 0, \pm1, \pm2, \ldots$

In this equation the chordwise integration is represented by

$$I^{(\bar m)}(x) = \frac{1}{\pi}\int_0^\pi \Phi(\bar m) e^{ix\cos\varphi_\alpha} d\varphi_\alpha \qquad (7a)$$

where $\Phi(\bar m)$ is the lift operator function and

$$\Lambda^{(\bar n)}(y) = \frac{1}{\pi}\int_0^\pi \Theta(\bar n) e^{-iy\cos\theta_\alpha} \sin\theta_\alpha d\theta_\alpha \qquad (7b)$$

where $\Theta(\bar n)$ is the chordwise mode shape selected. (See References 3,4,5,6.)

In Eq.(6) the kernel function

$$\sum_{m_4=-\infty}^{\infty} \bar K_{AA}^{(\bar m,\bar n)} \quad (m_4 = q_A + \ell_4 N_A)$$

is given by Eq.(7) with $q=q_A$, $N=N_A$, $r=r_A$ and $\rho=\rho_A$. However, $r_o=r_{FO}$ the radius of the forward propeller.

In Eq.(5) the kernel function

$$\sum_{m_1=-\infty}^{\infty} \bar K_{FF}^{(\bar m,\bar n)} \quad (m_1 = -q_F + \ell_1 N_F)$$

is also given by Eq.(7) but with $q=q_F$, $N=N_F$, $r=r_F$ and $\rho=\rho_F$. In both Eqs.(5) and (6), the radial positions r and ρ and the inverse advance ratio a are non-dimensionalized by forward propeller radius r_{FO}

The Kernels $\bar K_{AF}$ and $\bar K_{FA}$

These are the kernels of the cross-coupling terms of Eqs.(5) and (6). Let the distance between the propeller planes of the two units of the CR system be ε (in terms of r_{FO}). Then for a RH after propeller at a distance ε from a LH forward propeller operating at the same RPM, the derivations of Reference 3 can be reduced to the following final forms:

$$\bar K_{AF}^{(\bar m,\bar n)}(m_2 = q_F + \ell_2 N_A \ge 0) = \left\{\frac{-N_A}{4\pi\rho_f U^2 r_{FO}}\right\} \frac{r_F}{a\sqrt{1+a^2 r_F^2}} e^{im_2(2\sigma_4 + a\varepsilon)}$$

$$\cdot e^{iq_F(\sigma_F - \sigma_A - a\varepsilon)} \left\{A(0)B(0) - \frac{i}{\pi}\int_0^\infty [A(u)B(u) - A(-u)B(-u)]\frac{du}{u}\right\} \qquad (8)$$

where

$$A(u) = \begin{cases} I_{m_2}(|u - a(m_2 - q_F)|\rho_A) K_{m_2}(|u - a(m_2 - q_F)|r_F) & \text{for } \rho_A \le r_F \\ I_{m_2}(|u - a(m_2 - q_F)|r_F) K_{m_2}(|u - a(m_2 - q_F)|\rho_A) & \text{for } r_F < \rho_A \end{cases}$$

$$B(u) = \left[au - a^2(m_2 - q_F) - \frac{m_2}{r_F^2}\right]\left[au - a^2(m_2 - q_F) + \frac{m_2}{\rho_A^2}\right]$$

$$\cdot e^{iu(\sigma_F - \sigma_A - a\varepsilon)/a} I^{(\bar m)}\left((-q_F - \tfrac{u}{a})\theta_{bF}\right)$$

$$\cdot \Lambda^{(\bar n)}\left((2m_2 - q_F - \tfrac{u}{a})\theta_{bA}\right)$$

and

$$\bar K_{FA}^{(\bar m,\bar n)}(m_3 = q_A + \ell_3 N_F \ge 0) = \left\{\frac{-N_F}{4\pi\rho_f U^2 r_{FO}}\right\} \frac{r_A}{a\sqrt{1+a^2 r_A^2}} e^{-im_3(2\sigma_F - a\varepsilon)}$$

$$\cdot e^{-iq_A(\sigma_F - \sigma_A - a\varepsilon)} \left\{C(0)D(0) - \frac{i}{u}\int_0^\infty [C(u)D(u) - C(-u)D(-u)]\frac{du}{u}\right\} \qquad (9)$$

where

$$C(u) = \begin{cases} I_{m_3}(|u + a(m_3 - q_A)|\rho_F) K_{m_3}(|u + a(m_3 - q_A)|r_A) & \text{for } \rho_F \le r_A \\ I_{m_3}(|u + a(m_3 - q_A)|r_A) K_{m_3}(|u + a(m_3 - q_A)|\rho_F) & \text{for } r_A < \rho_F \end{cases}$$

$$D(u) = \left[au + a^2(m_3 - q_A) + \frac{m_3}{r_A^2}\right]\left[au + a^2(m_3 - q_A) - \frac{m_3}{\rho_F^2}\right]$$

$$\cdot e^{-iu(\sigma_F - \sigma_A - a\varepsilon)/a} I^{(\bar m)}\left((q_A - \tfrac{u}{a})\theta_{bA}\right)$$

$$\cdot \Lambda^{(\bar n)}\left((-2m_3 + q_A - \tfrac{u}{a})\theta_{bF}\right)$$

The kernels have been programmed with proper consideration being given to evaluating the finite contributions of the Cauchy-type singularities in the u-integrations at u=0 and of the Hadamard-type higher order singularities in the ρ-integrations when $\rho \to r$.

IV. THE NORMAL VELOCITIES

The LH sides of the integral equations represent the normal components of the velocity perturbations above that producing zero loading (lift) which corresponds to a rotating thin plate lying on the helicoidal surface of pitch angle (i.e., hydrodynamic pitch angle)

$$\beta = \tan^{-1}\frac{U}{\Omega r}$$

where U = forward speed, r = radial location of the corresponding helix. The perturbations considered are those due to hull wake (non-uniform inflow field), blade camber, incident flow angle, and also due to the thickness of the blades which mainly affect the velocity field around both propellers of the CR system. The effect of "nonplanar" thickness which contributes to the loading of both units is neglected as being small [5]. The effects of each of these imposed flows on the blade are calculated separately and simply added together as allowed by the linearity of the theory.

The left-hand sides of the integral equations due to the wake contribution can be harmonically analyzed and written in the form

$$W(r,\Theta) = \sum_{q=0} V_n(r) e^{-iq\Theta}$$

where Θ can be expressed in terms of the moving coordinator system attached to each propeller by $\Theta_F = \theta_{0F} - \Omega_F t$ and $\Theta_A = -\theta_{0A} + \Omega_A t$ for the case of the forward and after propeller, respectively, as shown in Figure 1. The normal wake velocities $V_n(r)$ can be determined from the harmonic analysis of the wake measurements, as shown in Reference 5. After the trigonometric transformation

$$\theta_o = \sigma - \theta_b \cos\theta_\alpha$$

and application of the "lift operator" of order $\bar m$

$$\frac{1}{\pi}\int_0^\pi \Phi(\bar m) W(r,\Theta) d\theta_\alpha$$

the following expressions result for the left-hand sides of the pair of integral equations relating the unknown loadings with the given "downwash" at each propeller:

$$\frac{\bar{W}_A^{(q_A,\bar{m})}(r_A)}{U} = \frac{V_A^{(q_A)}(r_A)}{U} e^{-iq_A\sigma_A} I^{(\bar{m})}(q_A\theta_{bA}) \quad (10)$$

for the after propeller, and

$$\frac{\bar{W}_F^{(q_F,\bar{m})}(r_F)}{U} = \text{conj}\left[\frac{V_F^{(q_F)}(r_F)}{U} e^{-iq_F\sigma_F} I^{(\bar{m})}(q_F\theta_{bF})\right]$$

for the forward propeller. It should be noted that the factor $\exp iq\Omega t$ has been omitted from the above expressions.

The velocities induced by the incident flow angle and camber effects are independent of time because the blades are considered rigid so that only the steady-state loadings will be affected.

For the flow angle (f) effects, the dimensionless perturbation velocities after the application of the lift operator become:

$$\left(\frac{\bar{W}_F^{(0,\bar{m})}(r_F)}{U}\right)_f = -\sqrt{1+a^2r_F^2}\left[\theta_{PF}(r_F)-\beta_F(r_F)\right] I^{(\bar{m})}(0) \quad (11)$$

and

$$\left(\frac{\bar{W}_A^{(0,\bar{m})}(r_A)}{U}\right)_f = -\sqrt{1+a^2r_A^2}\left[\theta_{PA}(r_A)-\beta_A(r_A)\right] I^{(\bar{m})}(0)$$

for the forward and after propellers, respectively, where θ_P is the blade pitch angle and β is the hydrodynamic pitch angle of the reference helicoidal surface (i.e., of zero loading).

For the camber (c) effect of the forward propeller, the dimensionless velocity ratio after the application of the lift operator becomes

$$\left(\frac{\bar{W}_F^{(0,\bar{m})}(r_F)}{U}\right)_c = \frac{\sqrt{1+a^2r_F^2}}{\pi}\int_0^{\pi} \Phi(\bar{m})\frac{\partial f(r_F,s_F)}{\partial s_F}\, d\varphi_\alpha \quad (12)$$

where

$f(r_F,s_F)$ = camberline ordinates as fraction of expanded chord length, measured from the face pitch line

$s_F = (1-\cos\varphi_\alpha)/2$, chordwise location non-dimensionalized on the basis of chord length

For the after propeller, the same expression is valid and only the subscript F must be replaced by A.

The evaluation of the integral of (12) is given in Reference 7 for arbitrary camber shape.

V. THE EFFECTS OF BLADE THICKNESS OF EACH PROPELLER ON THE VELOCITY FIELD OF THE OTHER

In addition to the disturbances of the velocity field about each propeller due to wake, its flow angle and camber, the disturbances considered are those due to the effects of the thickness of the blades of one propeller on the velocity incident on the other. These normal velocities on the LH side of the integral equations have been developed on the basis of "thin" body approximations [8]. Furthermore, it is assumed that the thickness distribution is approximated by a lenticular cross-section, an assumption which has been shown to be a good approximation for determining velocity and pressure [8,9] on a point in the neighborhood of an operating propeller as long as it is not a point on its blade and particularly near the leading edge. It should also be recalled that the velocity and pressure fields generated by an operating propeller even in a uniform inflow yields steady and unsteady components of the respective field. Thus although it is independent of time, the blade thickness produces both steady and unsteady components of the velocity field.

Following the same procedure as in Reference 8, it can be shown that the dimensionless velocity normal to the blades of the forward propeller induced by the after propeller thickness, with maximum thickness-chord ratio t_o/c, is given for $q_F = 0$ by

$$\left(\frac{\bar{W}_F^{(0,\bar{m})}(r_F)}{U}\right)_{tA} = -\frac{4a^3r_FN_A}{\pi^2\sqrt{1+a^2r_F^2}}\int_{\rho_A}\frac{\rho_A}{\theta_{bA}}\sqrt{1+a^2\rho_A^2}\,\frac{t_o}{c}(\rho_A)$$
$$\cdot\int_0^{\infty} u(IK)_o F(u,\rho_A)\,\text{R.P.}\left[e^{iu(\sigma_A-\sigma_F+a\epsilon)/a} I^{(\bar{m})}\left(\frac{u}{a}\theta_{bF}\right)\right]du\,d\rho_A \quad (13)$$

where

$$(IK)_o = \begin{cases} I_o(u\rho_A)K_o(ur_F) & \text{for } \rho_A < r_F \\ I_o(ur_F)K_o(u\rho_A) & \text{for } r_F < \rho_A \end{cases}$$

$$F(u,\rho_A) = \frac{\sin\frac{u\theta_{bA}}{a} - \frac{u\theta_{bA}}{a}\cos\left(\frac{u\theta_{bA}}{a}\right)}{u^2}$$

$I_o(\,)$ and $K_o(\,)$ are modified Bessel functions of first and second kind of order zero

and for $q_F = 2\ell N_A$ where $\ell = 1,2 \ldots$, by

$$\left(\frac{\bar{W}_F^{(2\ell N_A,\bar{m})}(r_F)}{U}\right)_{tA} = -\frac{4a^2r_FN_A}{\pi^2\sqrt{1+a^2r_F^2}} e^{-i\ell N_A(2\sigma_F-a\epsilon)}$$
$$\cdot\int_{\rho_A}\frac{\rho_A}{\theta_{bA}}\sqrt{1+a^2\rho_A^2}\,\frac{t_o}{c}(\rho_A)$$
$$\cdot\int_0^{\infty} F(u,\rho_A)\left[G(u)-G(-u)\right]du\,d\rho_A \quad (14)$$

where

$$G(u) = \left[au+\ell N_A\left(a^2-\frac{1}{r_F^2}\right)\right] I_{\ell N_A}(|u+a\ell N_A|\rho_A) K_{\ell N_A}(|u+a\ell N_A|r_F)$$
$$\cdot e^{iu(\sigma_A-\sigma_F+a\epsilon)/a} I^{(\bar{m})}\left((2\ell N_A+\frac{u}{a})\theta_{bF}\right)$$

for $\rho_A < r_F$. If $\rho_A > r_F$, these factors are interchanged in the modified Bessel functions.

The velocity normal to the blades of the after propeller induced by the forward propeller thickness is for $q_A = 0$

$$\left(\frac{\bar{W}_A^{(0,\bar{m})}(r_A)}{U}\right)_{tF} = \frac{-4a^3r_AN_F}{\pi^2\sqrt{1+a^2r_A^2}}\int_{\rho_F}\frac{\rho_F}{\theta_{bF}}\sqrt{1+a^2\rho_F^2}\,\frac{t_o}{c}(\rho_F)$$

(15)
[Cont'd]

$$\cdot \int_0^\infty u(IK)_o F(u,\rho_F)\,R.P.\left[e^{-iu(\sigma_A-\sigma_F+a\epsilon)/a} I_{\bar{m}}\left(\frac{u\theta_{bA}}{a}\right)\right] du d\rho_F \tag{15}$$

where

$$(IK)_o = \begin{cases} I_o(u\rho_F)K_o(ur_A) & \text{for } \rho_F < r_A \\ I_o(ur_A)K_o(u\rho_F) & \text{for } r_A < \rho_F \end{cases}$$

$$F(u,\rho_F) = \frac{\sin\frac{u\theta_{bF}}{a} - \frac{u\theta_{bF}}{a}\cos\frac{u\theta_{bF}}{a}}{u^2}$$

and for $q_A = 2\ell N_F$, $\ell = 1,2,\ldots$

$$\left(\frac{\bar{W}_A^{(2\ell N_F,\bar{m})}(r_A)}{U}\right)_{tF} = \frac{-4a^2 r_A^{N_F}}{\pi^2\sqrt{1+a^2 r_A^2}}\, e^{-i\ell N_F(2\sigma_F+a\epsilon)} \cdot \int_{\rho_F} \frac{\rho_F}{\theta_{bF}}\sqrt{1+a^2\rho_F^2}\;\frac{t_o}{c}(\rho_F) \cdot \int_0^\infty F(u,\rho_F)[N(u)-N(-u)]\,du d\rho_F \tag{16}$$

where

$$N(u) = \left[au + \ell N_F\left(a^2 - \frac{1}{r_A^2}\right)\right] I_{\ell N_F}(|u+a\ell N_F|\rho_F)\, K_{\ell N_F}(|u+a\ell N_F|r_A) \cdot e^{-iu(\sigma_A-\sigma_F+a\epsilon)/a} I_{\bar{m}}\left((2\ell N_F+\frac{u}{a})\theta_{bA}\right)$$

for $\rho_F < r_A$. If $\rho_F > r_A$, these factors are interchanged in the modified Bessel functions.

VI. SOLUTION OF THE PAIR OF INTEGRAL EQUATIONS

It is seen from Eqs.(5) and (6) that the loading on each propeller of the CR system is affected by all the harmonics of the inflow field. Here, however, the solution will be limited to the uniform inflow case, i.e., to the steady-state normal velocities due to camber (c) and to incident flow angle (f), and to the steady and unsteady effects of the interaction (i.e., cross-coupling terms) between the propellers and to their respective thicknesses.

Equation (5) becomes for each $\bar{m}$ and $\bar{n}$, for $q_F = 0$

$$\left[\frac{\bar{W}_F^{(0)}(r_F)}{U}\right]_{c+f+tA} = \int_{\rho_F} L_F^{(0)}(\rho_F)\bar{K}'_{FF}(q_F=0)\,d\rho_F + \int_{\rho_A}\left\{L_A^{(0)}(\rho_A)\bar{K}_{AF}(m_2=0) + L_A^{(2N_A)}(\rho_A)\bar{K}_{AF}(m_2=N_A) + \ldots\right\} d\rho_A \tag{17a}$$

and for $q_F = 2N_A$

$$\left[\frac{\bar{W}_F^{(2N_A)}(r_F)}{U}\right]_{tA} = \int_{\rho_F} L_F^{(2N_A)}(\rho_F)\bar{K}'_{FF}(q_F=2N_A)\,d\rho_F + \int_{\rho_A}\left\{L_A^{(0)}(\rho_A)\bar{K}_{AF}(m_2=N_A) + L_A^{(2N_A)}(\rho_A)\bar{K}_{AF}(m_2=2N_A) + \ldots\right\} d\rho_A \tag{17b}$$

Equation (6) becomes for each $\bar{m}$ and $\bar{n}$, for $q_A = 0$

$$\left[\frac{\bar{W}_A^{(0)}(r_A)}{U}\right]_{c+f+tF} = \int_{\rho_F}\left\{L_F^{(0)}(\rho_F)\bar{K}_{FA}(m_3=0) + L_F^{(2N_F)}(\rho_F)\bar{K}_{FA}(m_3=N_F) + \ldots\right\} d\rho_F + \int_{\rho_A} L_A^{(0)}(\rho_A)\bar{K}'_{AA}(q_A=0)\,d\rho_A \tag{18a}$$

and for $q_A = 2N_F$

$$\left[\frac{\bar{W}_A^{(2N_F)}(r_A)}{U}\right]_{tF} = \int_{\rho_F}\left\{L_F^{(0)}(\rho_F)\bar{K}_{FA}(m_3=N_F) + L_F^{(2N_F)}(\rho_F)\bar{K}_{FA}(m_3=2N_F) + \ldots\right\} d\rho_F + \int_{\rho_A} L_A^{(2N_F)}(\rho_A)\bar{K}'_{AA}(q_A=2N_F)\,d\rho_A \tag{18b}$$

where

$$\bar{K}'_{FF} = \sum_{m_1=-\infty}^{\infty}\bar{K}_{FF}$$

$$\bar{K}'_{AA} = \sum_{m_4=-\infty}^{\infty}\bar{K}_{AA}$$

(The higher frequencies are assumed negligible.)

Even in this simplified problem, a direct solution of the equations is impracticable; therefore an iteration procedure must be devised. It is assumed at first that the effect of the after propeller on the forward propeller (except for the thickness effect) is small and hence the second terms on the RH of Eqs.(17a) and (17b) may be omitted.

The iteration procedure is given below for two cases: for a CR system with equal number of blades (i.e., $N_F = N_A = N$) and for one with unequal number (i.e., $N_F \neq N_A$), and neither one is an integer multiple of the other.

Case #1: $N_F = N_A = N$

0-iteration (first)

1) $L_{F0}^{(0,\bar{n})}(\rho_F) = \left[\bar{K}'_{FF}(q_F=0)\right]^{-1} \cdot \left\{\left(\frac{\bar{W}_F^{(0,\bar{m})}(r_F)}{U}\right)_{c+f} + \left(\frac{\bar{W}_F^{(0,\bar{m})}(r_R)}{U}\right)_{tA}\right\}$

2) $L_{F0}^{(2N,\bar{n})}(\rho_F) = \left[\bar{K}'_{FF}(q_F=-2N)\right]^{-1} \cdot \left\{\left(\frac{\bar{W}_F^{(2N,\bar{m})}(r_F)}{U}\right)_{tA}\right\}$

where $\bar{K}'_{FF}(q_F) = \sum_{m_1=-\infty}^{\infty}\bar{K}_{FF}^{(\bar{m},\bar{n})}(m_1)$

3) $L_{A1}^{(0,\bar{n})}(\rho_A) = [\bar{K}'_{AA}(q_A=0)]^{-1} \cdot \left\{\left(\frac{\bar{W}_A^{(0,\bar{m})}(r_A)}{U}\right)_{c+f} + \left(\frac{\bar{W}_A^{(0,\bar{m})}(r_A)}{U}\right)_{tF} - \sum_{\rho_F}\left[L_{F0}^{(0,\bar{n})}\bar{K}_{FA}^{(\bar{m},\bar{n})}(m_3=0,\, q_A=0) + L_{F0}^{(2N,\bar{n})}\bar{K}_{FA}^{(\bar{m},\bar{n})}(m_3=N,\, q_A=0)\right]\right\}$

4) $L_{A1}^{(2N,\bar{n})}(\rho_A) = [\bar{K}'_{AA}(q_A=2N)]^{-1} \cdot \left\{ \left(\frac{\bar{W}_A^{(2N,\bar{m})}(r_A)}{U} \right)_{tF} \right.$

$- \sum_{\rho_f} \left[L_{F0}^{(0,\bar{n})} \cdot \bar{K}_{FA}^{(\bar{m},\bar{n})}(m_3=N,\ q_A=2N) \right.$

$\left. \left. L_{F0}^{(2N,\bar{n})} \cdot \bar{K}_{FA}^{(\bar{m},\bar{n})}(m_3=2N,\ q_A=2N) \right] \right\}$

where $\bar{K}'_{AA}(q_A) = \sum_{m_4=-\infty}^{\infty} \bar{K}_{AA}^{(\bar{m},\bar{n})}(m_4)$

1-iteration (second iteration)

1) $L_{F1}^{(0,\bar{n})}(\rho_F) = [\bar{K}'_{FF}(q_F=0)]^{-1} \left\{ \left(\frac{\bar{W}_F^{(0,\bar{m})}(r_F)}{U} \right)_{c+f} + \left(\frac{\bar{W}_F^{(0,\bar{m})}(r_F)}{U} \right)_{tA} \right.$

$- \sum_{\rho_A} \left[L_{A1}^{(0,\bar{n})} \cdot \bar{K}_{AF}^{(\bar{m},\bar{n})}(m_2=0, q_F=0) \right.$

$\left. \left. + L_{A1}^{(2N,\bar{n})} \cdot \bar{K}_{AF}^{(\bar{m},\bar{n})}(m_2=N,\ q_F=0) \right] \right\}$

2) $L_{F1}^{(2N,\bar{n})}(\rho_F) = [\bar{K}'_{FF}(q_F=-2N)]^{-1} \cdot \left\{ \left(\frac{\bar{W}_F^{(2N,\bar{m})}(r_F)}{U} \right)_{tA} \right.$

$- \sum_{\rho_A} \left[L_{A1}^{(0,\bar{n})} \cdot \bar{K}_{AF}^{(\bar{m},\bar{n})}(m_2=N,\ q_F=2N) \right.$

$\left. \left. + L_{A1}^{(2N,\bar{n})} \cdot \bar{K}_{AF}^{(\bar{m},\bar{n})}(m_2=2N,\ q_F=2N) \right] \right\}$

3) $L_{A2}^{(0,\bar{n})}(\rho_A) = [\bar{K}'_{AA}(q_A=0)]^{-1} \cdot \left\{ \left(\frac{\bar{W}_A^{(0,\bar{m})}(r_A)}{U} \right)_{c+f} + \left(\frac{\bar{W}_A^{(0,\bar{m})}(r_A)}{U} \right)_{tF} \right.$

$- \sum_{\rho_F} \left[L_{F1}^{(0,\bar{n})} \cdot \bar{K}_{FA}^{(\bar{m},\bar{n})}(m_3=0,\ q_A=0) \right.$

$\left. \left. + L_{F1}^{(2N,\bar{n})} \cdot \bar{K}_{FA}^{(\bar{m},\bar{n})}(m_3=N,\ q_A=0) \right] \right\}$

4) $L_{A2}^{(2N,\bar{n})}(\rho_A) = [\bar{K}'_{AA}(q_A=2N)]^{-1} \cdot \left\{ \left(\frac{\bar{W}_A^{(2N,\bar{m})}(r_A)}{U} \right)_{tF} \right.$

$- \sum_{\rho_f} \left[L_{F1}^{(0,\bar{n})} \cdot \bar{K}_{FA}^{(\bar{m},\bar{n})}(m_3=N,\ q_A=2N) \right.$

$\left. \left. + L_{F1}^{(2N,\bar{n})} \cdot \bar{K}_{FA}^{(\bar{m},\bar{n})}(m_3=2N,\ q_A=2N) \right] \right\}$

and so on, until values of loadings are stabilized.

Case #2: $N_A \neq N_F$

0-iteration (first)

1) $L_{F0}^{(0,\bar{n})}(\rho_F) = [\bar{K}'_{FF}(q_F=0)]^{-1} \cdot \left\{ \left(\frac{\bar{W}_F^{(0,\bar{m})}(r_F)}{U} \right)_{c+f+tA} \right\}$

2) $L_{F0}^{(2N_A,\bar{n})}(\rho_F) = [\bar{K}'_{FF}(q_F=-2N_A)]^{-1} \cdot \left\{ \left(\frac{\bar{W}_F^{(2N_A,\bar{m})}(r_F)}{U} \right)_{tA} \right\}$

3) $L_{A1}^{(0,\bar{n})}(\rho_A) = [\bar{K}'_{AA}(q_A=0)]^{-1} \cdot \left\{ \left(\frac{\bar{W}_A^{(0,\bar{m})}(r_A)}{U} \right)_{c+f+tF} \right.$

$\left. - \sum_{\rho_F} L_{F0}^{(0,\bar{n})} \cdot \bar{K}_{FA}^{(\bar{m},\bar{n})}(m_3=0,\ q_A=0) \right\}$

4) $L_{A1}^{(2N_F,\bar{n})}(\rho_A) = [\bar{K}'_{AA}(q_A=2N_F)]^{-1} \cdot \left\{ \left(\frac{\bar{W}_A^{(2N_F,\bar{m})}(r_A)}{U} \right)_{tF} \right.$

$\left. - \sum_{\rho_F} L_{F0}^{(0,\bar{n})} \cdot \bar{K}_{FA}^{(\bar{m},\bar{n})}(m_3=N_F,\ q_A=2N_F) \right\}$

where $\bar{K}'_{FF}(q_F) = \sum_{m_1=-\infty}^{\infty} \bar{K}_{FF}^{(\bar{m},\bar{n})}(m_1)$

and $\bar{K}'_{AA}(q_A) = \sum_{m_4=-\infty}^{\infty} \bar{K}_{AA}^{(\bar{m},\bar{n})}(m_4)$

1-iteration (second)

1) $L_{F1}^{(0,\bar{n})}(\rho_F) = [\bar{K}'_{FF}(q_F=0)]^{-1} \cdot \left\{ \left(\frac{\bar{W}_F^{(0,\bar{m})}}{U} \right)_{c+f+tA} \right.$

$\left. - \sum_{\rho_A} \left[L_{A1}^{(0,\bar{n})} \cdot \bar{K}_{AF}^{(\bar{m},\bar{n})}(m_2=0,\ q_F=0) \right] \right\}$

2) $L_{F1}^{(2N_A,\bar{n})}(\rho_F) = [\bar{K}'_{FF}(q_F=-2N_A)]^{-1} \cdot \left\{ \left(\frac{\bar{W}_F^{(2N_A,\bar{n})}(r_F)}{U} \right)_{tA} \right.$

$\left. - \sum_{\rho_A} \left[L_{A1}^{(0,\bar{n})} \cdot \bar{K}_{AF}^{(\bar{m},\bar{n})}(m_2=N_A, q_F=2N_A) \right] \right\}$

3) $L_{A2}^{(0,\bar{n})}(\rho_A) = [\bar{K}'_{AA}(q_A=0)]^{-1}$

$\left\{ \left(\frac{\bar{W}_A^{(0,\bar{m})}(r_A)}{U} \right)_{c+f+tF} \right.$

$\left. - \sum_{\rho_F} \left[L_{F1}^{(0,\bar{n})} \cdot \bar{K}_{FA}^{(\bar{m},\bar{n})}(m_3=0,\ q_A=0) \right] \right\}$

4) $L_{A2}^{(2N_F,\bar{n})}(\rho_A) = [\bar{K}'_{AA}(q_A=2N_F)]^{-1}$

$\cdot \left\{ \left(\frac{\bar{W}_A^{(2N_F,\bar{m})}(r_A)}{U} \right)_{tF} \right.$

$\left. - \sum_{\rho_F} \left[L_{F1}^{(0,\bar{n})} \cdot \bar{K}_{FA}^{(\bar{m},\bar{n})}(m_3=N_F,\ q_A=2N_F) \right] \right\}$

and so on, until values of loadings are stabilized.

It is to be noted that, in contrast to the case of equal number of blades for the two propellers of the CR system, when the propellers have an unequal number of blades, $N_A \neq N_F$, the series representing the cross-coupling terms due to the interaction effects are more limited. As will be shown later, for this case there is no unsteady loading L_F on the forward propeller at frequency $2N_F$ and no unsteady loading L_A on the after propeller at frequency $2N_A$. It should be kept in mind that the iteration scheme has been restricted to the lowest possible frequencies of the interacting CR system. It will be easily generalized by means of Eqs.(5) and (6) by varying parameters ℓ_1, ℓ_2, ℓ_3, ℓ_4 (all integers) to other values than those already used (0, ±1).

VII. PROPELLER LOADING AND RESULTING HYDRODYNAMIC FORCES AND MOMENTS

Propeller Loading

Once the values of $L^{(q,\bar{n})}(r)$, the spanwise loading components, or coefficients of the chordwise distribution, are obtained, the spanwise loading distribution $L^{(q)}(r)$ is determined as [5,6]:

$$L^{(q)}(r) = \int_0^{\pi} \sum_{\bar{n}=1}^{\bar{n}max} L^{(q,\bar{n})}(r)\Theta(\bar{n})\sin\theta_\alpha d\theta_\alpha \qquad (19)$$

where $\Theta(\bar{n})$ = chordwise modes. Because the interaction phenomenon introduces an angle of attack even in the steady-state case $\Theta(\bar{n})$ is taken as the complete Birnbaum series which has the proper leading edge singularity and satisfies the Kutta condition at the trailing edge. In this case it can be shown that

$$L^{(q)}(r) = L^{(q,1)}(r) + \frac{1}{2} L^{(q,2)}(r) \qquad (19a)$$

Hydrodynamic Forces and Moments

The principal components of these forces and moments which are evaluated for each member of the CR system are listed below and shown in Figure 2 for a RH propeller with the sign convention adopted.

Forces: F_x=thrust (x-direction)
F_y and F_z=horizontal and vertical components, respectively, of the bearing forces

Moments: Q_x=torque about the x-axis
Q_y and Q_z=bending moments about the y- and z-axis, respectively

(Subscripts F and A added to these symbols will designate forward and after propeller cases.)

The elementary forces and moments can be determined by resolving the chordwise loadings, acting on an elementary radial strip, normal to the strip and taking the corresponding moments about any axis as in Reference 5. However, for simplification of the discussion which follows, the assumption will be made, as in Reference 10, that the spanwise loading $L^{(q)}(r)$ acts at the midchord. This is exactly the case as far as thrust and torque are concerned and a good approximation for the transverse bearing forces and bending moments if the blades are not wide, which is the case with counterrotating propellers.

Thus the elementary forces acting at radius r of an N-bladed propeller will be given by

$$\Delta F_x = \sum_{n=1}^{N} L^{(q)}(r) e^{iq(\Omega t+\bar{\theta}_n)} \cos\theta_p(r)\Delta r$$

$$\Delta F_y = \sum_{n=1}^{N} L^{(q)}(r) e^{iq(\Omega t+\bar{\theta}_n)} \sin\theta_p(r)\cos(\Omega t+\bar{\theta}_n)\Delta r$$

$$\Delta F_z = -\sum_{n=1}^{N} L^{(q)}(r) e^{iq(\Omega t+\bar{\theta}_n)} \sin\theta_p(r)\sin(\Omega t+\bar{\theta}_n)\Delta r \qquad (20)$$

where $\theta_p(r)$ is the geometric pitch angle at radius r and $\bar{\theta}_n = 2\pi(n-1)/N, n=1,2,\ldots N$. The elementary moments will be given by

$$\Delta Q_x = -\sum_{n=1}^{N} rL^{(q)}(r) e^{iq(\Omega t+\bar{\theta}_n)} \sin\theta_p(r)\Delta r$$

$$\Delta Q_y = \sum_{n=1}^{N} rL^{(q)}(r) e^{iq(\Omega t+\bar{\theta}_n)} \cos\theta_p(r)\cos(\Omega t+\bar{\theta}_n)\Delta r$$

$$\Delta Q_z = -\sum_{n=1}^{N} rL^{(q)}(r) e^{iq(\Omega t+\bar{\theta}_n)} \cos\theta_p(r)\sin(\Omega t+\bar{\theta}_n)\Delta r \qquad (21)$$

The summation over all the blades of a propeller involves

1) for thrust and torque

$$\sum_{n=1}^{N} e^{iq\bar{\theta}_n} = \begin{cases} N \text{ when } q=nN,\ n=0,1,2\ \ldots \\ 0 \text{ for all other } q \end{cases} \qquad (22)$$

2) for transverse forces and bending moments

$$\sum_{n=1}^{N} e^{i(q\pm1)\bar{\theta}_n} = \begin{cases} N \text{ when } q=nN\mp1,\ n=0,1,2\ \ldots \\ 0 \text{ for all other } q \end{cases} \qquad (23)$$

It is thus evident that in the steady-state case (q=0) thrust and torque from each propeller will be present (see Eq.22), whereas, since the condition under consideration is that of uniform inflow into the forward propeller, there will be no transverse forces and bending moments (see Eq.23). This will be so whether the propellers are of equal or unequal number of blades.

As has been shown the interaction phenomenon induces unsteady loadings on both units of the CR system. In the case of equal blade number, those on the forward propeller are $L_F^{(2\ell N)}(r_F)$, on the after propeller, $L_A^{(2\ell N)}(r_A)$. As seen from Eqs.(22) and (23) both propellers generate thrust and torque at frequencies $q = 2\ell N, \ell=1,2, \ldots$, which corresponds to blade-blade crossing frequency for such propellers, and no unsteady transverse bearing forces and moments, since no combination of integers ℓ and n can satisfy the relation $(2\ell-n)N=\mp1$.

In the case of unequal blade number, $N_A \neq N_F$, the unsteady loadings on the forward propeller are at frequencies $q_F=2\ell_1 N_A$ and $2\ell_2 N_F$ and on the after propeller at $q_A=2\ell_3 N_F$ and $2\ell_4 N_A$. The criterion for thrust and torque, Eq.(22), yields

$$\begin{aligned} q_F &= 2\ell_1 N_A = n_1 N_F \\ q_F &= 2\ell_2 N_F = n_2 N_F \\ q_A &= 2\ell_3 N_F = n_3 N_A \\ q_A &= 2\ell_4 N_A = n_4 N_A \end{aligned} \qquad (22a)$$

and the criterion for transverse forces and bending moments, Eq.(23), yields

$$q_F = 2\ell_1 N_A = n_1 N_F \mp 1$$
$$q_F = 2\ell_3 N_F \neq n_3 N_F \mp 1$$
$$q_A = 2\ell_3 N_F = n_3 N_A \mp 1$$
$$q_A = 2\ell_4 N_A \neq n_4 N_A \mp 1 \qquad (23a)$$

The conditions of (22a) for thrust and torque are always satisfied for frequency $q=q_F=q_A$ by choosing $\ell_1=\ell_4=mN_F$, $\ell_3=\ell_3=mN_A$, $m=1,2,\ldots$, so that $q = 2mN_AN_F$, i.e., the so-called blade-blade crossing frequency and multiples thereof. Equation (22a) can also be satisfied at lower frequencies (1) if $N_A=kN_F$, k being an integer, in which case choosing $\ell_1 k = \ell_2 = \ell_3 = \ell_4 k$ yields $q = 2mkN_F$, and (2) if N_A and N_F are both even numbers, in which case $q = mN_AN_F$. In the latter two cases the conditions of (23a) for transverse forces and bending moments are obviously not satisfied.

When $N_A \neq kN_F$ and N_A and N_F are not both even numbers, the CR system generates thrust and torque only at $q = 2mN_AN_F$ (blade-blade crossing frequencies).

The conditions of (23a) are satisfied for

$$q = q_F \mp 1 = 2\ell_1 N_A \mp 1 = n_1 N_F$$
$$q = q_A \pm 1 = 2\ell_3 N_F \pm 1 = n_3 N_A$$

since $2\ell_1 N_A + 2\ell_3 N_F = n_3 N_A + n N_F$ is possible. The frequencies at which side forces and bending moments of the CR system occur are

$$q = 2\ell_1 N_A \mp 1 = 2\ell_3 N_F \pm 1$$

from which $2\ell_1 N_A = 2\ell_3 N_F \pm 2$.

An easy way of determining the frequencies for alternating forces and moments is to write out the sequence of numbers which are integer multiples of twice the blade number. For example, for 3 and 5 blades

3: 6 12 18 24 30 ...

5: 10 20 30 ...

The frequencies for side forces will be the mean of any pair of numbers in the two sequences which differ by 2, in this case 11, 19 ... . The frequencies for thrust and torque will be the mean of any pair of numbers which are alike, in this case 30,60... . For 6 and 4 blades, the two lowest frequencies will be 24 and 48 for thrust and torque. (There is no side force in this case.)

Another derivation of the frequencies of the alternating forces developed by interactions between a pair of counterrotating propellers in a uniform inflow is given by Reference 11, with the same results.

On the basis of the preceding discussion, the total forces and moments are obtained from (20) and (21) as;

1) for thrust and torque

$$(F_x)_F = N_F r_o e^{iq\Omega t} \int_0^1 L_F^{(q)}(r_F)\cos\theta_p(r_F)\,dr_F$$

$$(F_x)_A = N_A r_o e^{iq\Omega t} \int_0^1 L_A^{(q)}(r_A)\cos\theta_p(r_A)\,dr_A \qquad (24a)$$

$$(Q_x)_F = -N_F r_o^2 e^{iq\Omega t} \int_0^1 L_F^{(q)}(r_F)\sin\theta_p(r_F)\,r_F\,dr_F$$

$$(Q_x)_A = -N_A r_o^2 e^{iq\Omega t} \int_0^1 L_A^{(q)}(r_A)\sin\theta_p(r_A)\,r_A\,dr_A \qquad (24b)$$

where $q=0$ for steady state, and the lowest frequency of the alternating thrust and torque is

$q = 2kN_F$ when $N_A=kN_F$, $k=1,2,\ldots$

$q = N_AN_F$ when $N_A\neq N_F$ and both are even numbers

$q = 2N_AN_F$ for all other $N_A\neq N_F$

2) for transverse bearing forces and bending moments, when $N_A\neq kN_F$ and N_A and N_F are not both even numbers,

$$(F_y)_F = \frac{N_F}{2} r_o e^{i(q_F\mp 1)\Omega t} \int_0^1 L_F^{(q_F)}(r_F)\sin\theta_p(r_F)\,dr_F$$

$$(F_z)_F = \mp i(F_y)_F$$

$$(F_y)_A = \frac{N_A}{2} r_o e^{i(q_A\pm 1)\Omega t} \int_0^1 L_A^{(q_A)}(r_A)\sin\theta_p(r_A)\,dr_A$$

$$(F_z)_A = \pm i(F_y)_A \qquad (25a)$$

$$(Q_y)_F = \frac{N_F}{2} r_o^2 e^{i(q_F\mp 1)\Omega t} \int_0^1 L_F^{(q_F)}(r_F)\cos\theta_p(r_F)\,r_F\,dr_F$$

$$(Q_z)_F = \mp i(Q_y)_F$$

$$(Q_y)_A = \frac{N_A}{2} r_o^2 e^{i(q_A\pm 1)\Omega t} \int_0^1 L_A^{(q_A)}(r_A)\cos\theta_p(r_A)\,r_A\,dr_A$$

$$(Q_z)_A = \pm i(Q_y)_A \qquad (25b)$$

where the upper signs (at $q=q_F-1=q_A+1$) are used when $N_A > N_F$ and the lower signs (at $q=q_F+1=q_A-1$) are used when $N_A < N_F$, and $q_F=2\ell_1 N_A$ and $q_A=2\ell_3 N_F$ where ℓ_1 and ℓ_3 must satisfy the condition $2\ell_1 N_A = 2\ell_3 N_F \pm 2$.

It is to be noted that $r_o=r_{Fo}$ = forward propeller radius and r_A and r_F are fractions of r_{Fo}, and that finally the real parts of the forces and moments are to be taken.

Blade Bending Moment

Following Reference 6, the blade bending moment about the face pitch line at any radius r_j of a blade of the forward or after propeller is calculated from the spanwise loading $L^{(q)}(r)$ at any shaft frequency q as

$$M_b^{(q)} = r_o^2 e^{iq\Omega t} \int_{r_j}^1 L^{(q)}(r)\cos[\theta_p(r)-\theta_p(r_j)](r-r_j)\,dr \qquad (26)$$

The instantaneous blade bending moment distribution

as the blades swing around the shaft is

$$M_b = \mathrm{Re} \sum_q M_b^{(q)} e^{iq\Omega t} \qquad (27)$$

Here $q=q_F$ for the forward propeller and $q=q_A$ for the after propeller.

VIII. NUMERICAL RESULTS

On the basis of the theoretical procedures outlined in the preceding sections, a numerical approach has been established and adapted to the CDC-6600 or 7600 high-speed digital computer. The program furnishes in the case of uniform inflow to the forward propeller, a) the steady and time-dependent blade loadings, b) the corresponding hydrodynamic forces and moments, and c) the blade bending moment about the face-pitch line at any radius.

The expressions for the kernel functions given by Eqs.(7-9), those for the normal velocities on the left-hand sides of the integral equations given by Eqs.(11-16), and the pair of integral equations (17a,b and 18a,b), constitute the desired working forms. The computer program prepares all the necessary information for the execution of the suggested iteration procedure. It is a lengthy program, the duration depending on the number of blades of each component of the CR system, on the number of selected chordwise modes, and the number of frequencies for which information will be desired.

To establish the accuracy and usefulness of the computational procedure, a correlation with existing experimental results must be made. Calculations have been performed for two CR configurations for which data are available from tests at David Taylor NSRDC [12,13]. The data are for the two lowest frequencies, $\ell_i=0$ and $\ell_i=1$, and the computations have been limited to these frequencies.

The iterative procedure starts after all the required information has been computed and stored properly. The necessary kernel functions and inverse kernel functions are calculated for both a 4-0-4 and a 4-0-5 CR system for values of m and q as indicated in the table below.

TABLE 1

4-0-4 CR System				4-0-5 CR System			
Matrix	Inverse Matrix	m	q	Matrix	Inverse Matrix	m	q
K_{AF}		0	0	K_{AF}		0	0
K_{AF}		4	0				
	K_{FF}		0		K_{FF}		0
K_{AF}		4	8	K_{AF}		5	10
K_{AF}		8	8				
	K_{FF}		-8		K_{FF}		-10
K_{FA}		0	0	K_{FA}		0	0
K_{FA}		4	0				
	K_{AA}		0		K_{AA}		0
K_{FA}		4	8	K_{FA}		4	8
K_{FA}		8	8				
	K_{AA}		8		K_{AA}		8

A workable program has been established which indicates that the number of iterations need not be greater than 10, although the execution time of an additional iteration is minimal.

The 4-0-4 CR system is composed of the David Taylor NSRDC propeller 3686 forward and propeller 3687-A aft, and the 4-0-5 set of propeller 3686 forward and propeller 3849 aft [13]. Propeller characteristics and flow conditions are given in the following table.

TABLE 2

	Propeller 3686	Propeller 3687-A	Propeller 3849
Number of Blades, N	4	4	5
EAR	0.303	0.322	0.379
P/D at 0.7R	1.291	1.320	1.267
Diameter, D, in	12.017	11.776	11.785
Rotation	L.H.*	R.H.*	R.H.*
n, rps	12	12	12
Speed, ft/sec	13.22	13.22	13.22
Advance rate, J	1.1**	1.1**	1.1**

*L.H. rotation is ccw looking forward
R.H. rotation is cw looking forward

**J based on diameter of forward propeller 3686

The theoretical predictions with and without thickness effects and the experimental results are summarized in the following table.

TABLE 3

CORRELATION OF PREDICTED AND MEASURED VALUES
4-0-4 CR SYSTEM

Forward Propeller 3686
After Propeller 3687-A
Axial Spacing = 0.28 forward propeller radius
J=1.1

		THEORY Without Thickness	THEORY With Thickness	EXPERIMENT
Q = 0 , Steady State				
Forward	$(\bar{K}_T)_F$	0.126*	0.1639*	0.125
Forward	$(\bar{K}_Q)_F$	0.0295*	0.0373*	0.0315
After	$(\bar{K}_T)_A$	0.145*	0.1335*	0.150
After	$(\bar{K}_Q)_A$	0.0330*	0.0308*	0.0315
Q = 2N = 8				
Forward	$(\bar{K}_T)_F$	0.0485	0.0747	0.0285
Forward	$(\bar{K}_Q)_F$	0.0101	0.0154	0.0058
After	$(\bar{K}_T)_A$	0.1156	0.1524	0.0095
After	$(\bar{K}_Q)_A$	0.0242	0.0312	0.0022

*Including friction

TABLE 4

CORRELATION OF PREDICTED AND MEASURED VALUES
4-0-5 CR SYSTEM

Forward Propeller 3686
After Propeller 3849
Axial Spacing=0.28 forward propeller radius
J = 1.1

Q = 0, Steady State

	THEORY		EXPERIMENT
	Without Thickness	With Thickness	
Forward $(\bar{K}_T)_F$	0.087*	0.1060*	0.130
Forward $(\bar{K}_Q)_F$	0.0207*	0.0246*	0.030
After $(\bar{K}_T)_A$	0.161*	0.1093*	0.130
After $(\bar{K}_Q)_A$	0.0361*	0.0255*	0.028
$Q_F = 2N_A-1=9$			
Forward $(\tilde{K}_{FH})_F$	0.0079	0.0239	0.0075
Forward $(\tilde{K}_{FV})_F$	0.0079	0.0239	0.0074
Forward $(\tilde{K}_{QH})_F$	0.0062	0.0053	0.0040
Forward $(\tilde{K}_{QV})_F$	0.0062	0.0053	0.0041
$Q_A = 2N_F+1=9$			
After $(\tilde{K}_{FH})_A$	0.0231	0.0275	0.0057
After $(\tilde{K}_{FV})_A$	0.0231	0.0275	0.0046
After $(\tilde{K}_{QH})_A$	0.0159	0.0181	0.0023
After $(\tilde{K}_{QV})_A$	0.0159	0.0181	0.0023

*Including friction

IX. CONCLUSIONS

Linearized unsteady lifting-surface theory has been applied in the study of two interacting propellers of a counterrotating system, when both units operate in a spatially non-uniform inflow. A mathematical model is introduced taking into account the exact geometry of the propulsive system as well as the three-dimensional spatially varying inflow. The propeller blades are considered to be of finite thickness and lying on a helicoidal surface of varying pitch. The blades have arbitrary planform, camber and sweep angle.

The computational procedure, however, has been developed and adapted to the CDC 6600 and 7600 high-speed digital computer, for the case where both units operate with the same RPM in a uniform inflow field.

The uniformity of the inflow field provides for a better understanding of the mechanism of interaction of the CR system, since the presence of wake harmonics would have such a dominant effect as to mask the interaction phenomenon.

The study provides information about the steady and unsteady blade loading distributions and the corresponding hydrodynamic forces and moments on both components of the propulsive device.

Rules have been established for the presence or absence of the steady and unsteady hydrodynamic forces and moment when the CR system is made up of equal and unequal numbers of blades. In fact, when the propellers of the CR system have equal number of blades, only the steady and unsteady thrust and torque will be generated on each propeller of the CR system, at zero and blade-blade crossing frequencies or multiples thereof ($q=2\ell N$, $\ell=1,2,3$ ... and N=common number of blades). When the CR system is made up of propellers with unequal number of blades, i.e., $N_F \neq N_A$, there is an easy way of determining the frequencies of alternating (unsteady) forces and moments.

The numerical work has been limited. The calculations without thickness effect have shown a reverse trend to that of experiment for the unsteady forces and moments generated on the after propeller. The numerical calculations have shown much higher values for the forces and moments exerted on the after propeller than those on the forward propeller. It is difficult to explain the discrepancy until more detailed and exhaustive numerical calculations are performed (including thickness effect). Furthermore, additional experimental work should also be conducted.

Some remarks are in order on the discrepancies between theory and experiment.

1) A few years ago an attempt was made to calculate unsteady thrust and torque of a counterrotating propeller system by a strip-wise method following the Kemp and Sears approach for the mutual interference of blades in cascade due to relative motion of successive blade rows. Results of this study have shown that the unsteady thrust of the after propeller is much higher than that of the forward propeller, when the bound vorticity and the vortex wake shed by the forward propeller are taken into account, either with flat plate modes or with an elliptic distribution.
2) Furthermore, observation of Dr. Wereldsma's experimental results (although these are for non-uniform inflow conditions), especially of the time records of the horizontal and vertical blade bending moments, show that superimposed on the fluctuations due to the wake at blade frequency, are the fluctuations due to blade interference at blade-blade crossing frequency. It can be seen that these fluctuations due to interference are much larger for the after propeller than for the forward.

The question of the discrepancies thus cannot be considered a closed subject, but requires further investigation both theoretical and experimental.

REFERENCES

1. Hadler, J.B., Morgan, W.B. and Meyers, K.A., "Advanced Propeller Propulsion for High-Powered Single-Screw Ships," Transactions SNAME, Vol.72, 1964.
2. Wereldsma, R., "Investigations on the Vibratory Output of Contrarotating Screw Propellers," 7th Symposium on Naval Hydrodynamics, Rome, August 25-30, 1968.
3. Tsakonas, S. and Jacobs, W.R., "Counterrotating and Tandem Propellers Operating in Spatially Varying, Three-Dimensional Flow Fields, Part I — Analysis," DL Report 1335, Stevens Institute of Technology, September 1968.
4. Jacobs, W.R. and Tsakonas, S., "A New Procedure for the Solution of Lifting Surface Problems," J. Hydronautics, Vol.3, No.1, January 1969.
5. Tsakonas, S., Jacobs, W.R. and Ali, M.R., "Propeller Blade Pressure Distribution Due to Loading and Thickness Effects," DL Report 1869, Stevens Institute of Technology, in

6. Tsakonas, S., Jacobs, W.R. and Ali, M.R., "An Exact Linear Lifting-Surface Theory for a Marine Propeller in a Non-Uniform Flow Field," DL Report 1509, Stevens Institute of Technology, February 1972; J.Ship Research, Vol.17, No.4, December 1973.

7. Tsakonas, S. and Jacobs, W.R., "Propeller Loading Distributions," DL Report 1319, Stevens Institute of Technology, August 1968; J. Ship Research, Vol.13, No.4, December 1969.

8. Jacobs, W.R. and Tsakonas, S., "Propeller-Induced Velocity Field Due to Thickness and Loading Effects; Report SIT-DL-73-1681, Stevens Institute of Technology, July 1973; J. Ship Research, Vol.19, No.1, March 1975.

9. Jacobs, W.R., Mercier, J. and Tsakonas, S, "Theory and Measurements of the Propeller-Induced Vibratory Pressure Field," Report SIT-DL-70-1485, Stevens Institute of Technology, December 1970; J. Ship Research, Vol.16, No.2, June 1972.

10. Tsakonas, S., Breslin, J.P. and Miller, M., "Correlation and Application of an Unsteady Flow Theory for Propeller Forces," Transactions, SNAME, Vol.75, 1967.

11. Strasberg, M. and Breslin, J.P., "The Frequencies of the Alternating Forces Due to Interactions of Contrarotating Propellers," to be published in J. Hydronautics, April 1976.

12. Hecker, R. and McDonald, N.A., "The Effect of Axial Spacing and Diameter on the Powering Performance of Counterrotating Propellers," David Taylor Model Basin Report 1342, February 1960.

13. Miller, M.L., "Experimental Determination of Unsteady Forces on Contrarotating Propellers in Uniform Flow," David W. Taylor Naval Ship Research and Development Center Report SPD-659-01, May 1976.

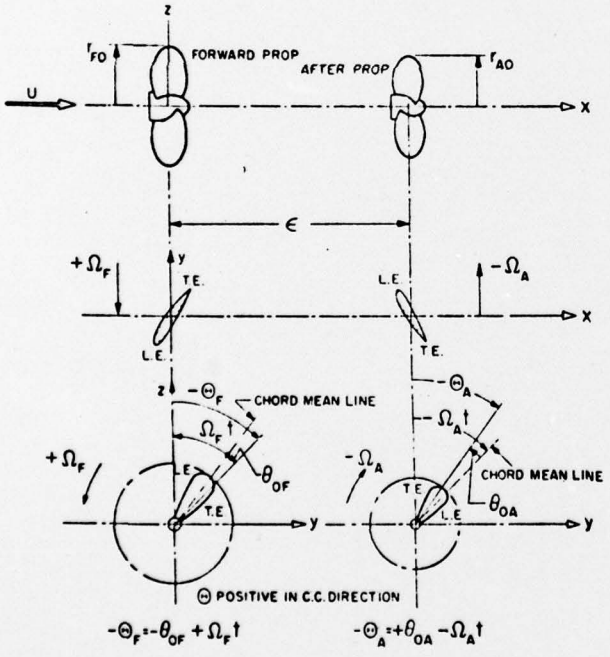

Fig. 1: Counterrotating propeller arrangement – angular coordinates.

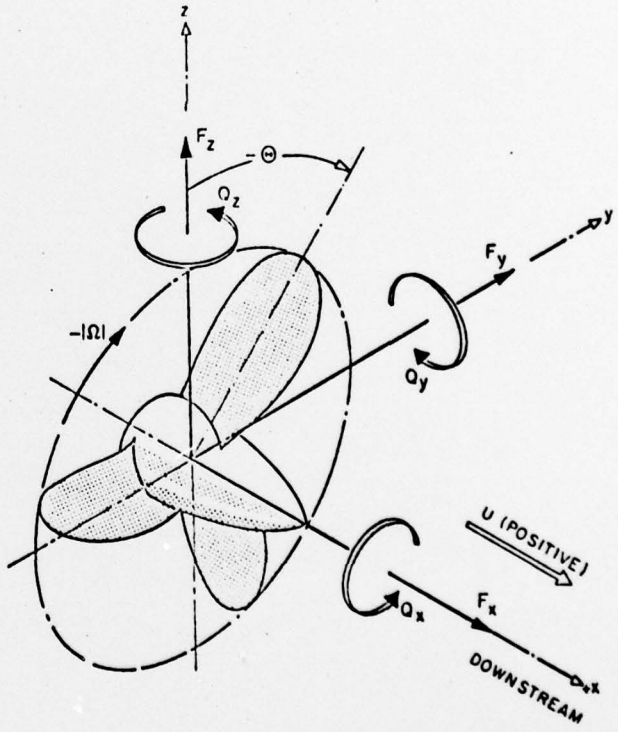

Fig. 2: Resolution of forces and moments.

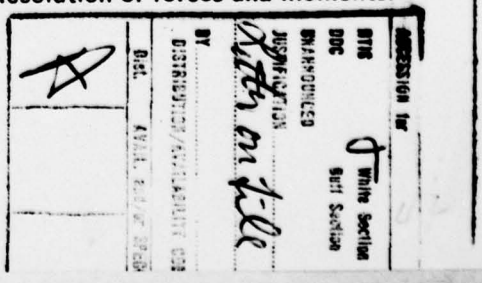

APPENDIX A

Effect of Blade Thickness of Each Propeller on the Velocity Field of the Other

1. The thickness distribution of a blade section is represented by a source-sink distribution assumed to be smeared over a projection of the section in the propeller plane. The velocity potential due to blade thickness of the after propeller at a point (x_F, r_F, φ_F) on the forward propeller is then given by

$$\left(\Phi_F(x_F, r_F, \varphi_F; t)\right)_{tA} = -\frac{1}{4\pi} \sum_{n=1}^{N_A} \int_{-\theta_{bA}}^{\theta_{bA}} \int_{\rho_A} \frac{M(\xi'_A, \rho_A, \theta_{A0})}{R_{AF}} \frac{\sqrt{1+a^2\rho_A^2}}{a\rho_A} \rho_A d\rho_A d\theta_{A0} \quad (A\text{-}1)$$

where $M(\xi'_A, \rho_A, \theta_{A0}) = \dfrac{2U\partial f(\xi'_A, \rho_A, \theta_{A0})}{\partial \xi'_A}$ source strength density determined in accordance with the "thin body" approach,

$f(\xi'_A, \rho_A, \theta_{A0})$ = thickness distribution over one side of the blade section at radial distance ρ_A in the propeller plane

$$R_{AF} = \left\{(x_F - \xi'_A)^2 + r_F^2 + \rho_A^2 - 2r_F\rho_A \cos[\theta_{A0} + \varphi_{F0} - 2\Omega t + \bar{\theta}_{An}]\right\}^{1/2}$$

$$x_F = \varphi_{F0}/a = (\sigma_F - \theta_{bF}\cos\varphi_\alpha)/a$$

$$\xi'_A = \theta_{A0}/a + \epsilon = (\sigma_A - \theta_{bA}\cos\theta_\alpha)/a + \epsilon$$

$$\bar{\theta}_{An} = (2\pi/N_A)(n-1), \quad n = 1, 2, \ldots N_A$$

Since $\dfrac{\partial f}{\partial \xi'} = \dfrac{a}{\theta_{bA}\sin\theta_\alpha} \dfrac{\partial f}{\partial \theta_\alpha}$

Eq. (A-1) can be reduced to

$$(\Phi_F)_{tA} = -\frac{U}{2\pi} \sum_{n=1}^{N_A} \int_0^{\pi} \int_{\rho_A} \frac{\partial f(\rho_A, \theta_\alpha)}{\partial \theta_\alpha} \frac{\sqrt{1+a^2\rho_A^2}}{R_{AF}} \partial\rho_A \, \partial\theta_\alpha \quad (A\text{-}2)$$

The thickness distribution $f(\rho_A, \theta_\alpha)$ will be approximated by a lenticular section, i.e.,

$$f(\rho_A, \theta_\alpha) \approx \frac{\tau(\rho_A)}{2} \sin^2\theta_\alpha$$

$$\approx \frac{t_o}{c}(\rho_A) \cdot \rho_A \theta_{bA} \sin^2\theta_\alpha \qquad \text{(A-3)}$$

where τ is maximum thickness in the projected plane, t_o/c is ratio of maximum thickness to chord of the expanded section, and $\rho_A \theta_{bA}$ is projected semichord. In addition, the reciprocal of the Descartes distance R_{AF} is expanded as

$$\frac{1}{R_{AF}} = \frac{1}{\pi} \sum_{m=-\infty}^{\infty} e^{im\beta} \int_{-\infty}^{\infty} (IK)_m \, e^{i(x_F - \xi'_A)k} \, dk \qquad \text{(A-4)}$$

where $\beta = \theta_{A0} + \varphi_{F0} - 2\Omega t + \bar{\theta}_{An}$

and $(IK)_m = \begin{cases} I_m(|k|\rho_A)\, K_m(|k|r_F) \text{ for } \rho_A < r_F \\ I_m(|k|r_F)\, K_m(|k|\rho_A) \text{ for } \rho_A > r_F \end{cases}$

With $\sum_{n=1}^{N_A} e^{im\bar{\theta}_{An}} = \begin{cases} N_A \text{ if } m = \ell N_A, \ \ell = 0, \pm 1, \pm 2, \ldots \\ 0 \text{ otherwise} \end{cases}$

and $\frac{\partial f}{\partial \theta_\alpha} \approx 2 \frac{t_o}{c}(\rho_A) \cdot \rho_A \theta_{bA} \sin\theta_\alpha \cos\theta_\alpha$

the velocity potential (A-2) becomes

$$(\Phi_F)_{tA} \approx -\frac{UN_A}{\pi^2} \sum_{\substack{m=-\infty \\ m=\ell N_A}}^{\infty} e^{-i2m\Omega t} \, e^{im(\varphi_{F0} + \sigma_A)}$$

$$\cdot \int_0^{\pi} \int_{\rho_A} e^{-im\theta_{bA}\cos\theta_\alpha} \sin\theta_\alpha \cos\theta_\alpha \rho_A \theta_{bA} \frac{t_o}{c}(\rho_A) \sqrt{1 + a^2\rho^2 A}$$

$$\cdot \int_{-\infty}^{\infty} (IK)_m \, e^{i(x_F - \xi'_A)k} \, dk \, d\rho_A \, d\theta_\alpha \qquad \text{(A-5)}$$

The velocity normal to the forward propeller blade due to the thickness of the after propeller, which is an additional perturbation on the L.H. of the first integral equation, is derived as

$$(W_F)_{tA} = -\frac{\partial}{\partial n'_F}(\Phi_F)_{tA} = -\frac{r_F}{\sqrt{1+a^2r_F^2}}\left(a\frac{\partial}{\partial x_F} - \frac{1}{r_F^2}\frac{\partial}{\partial \varphi_{F0}}\right)(\Phi_F)_{tA}$$

Therefore,

$$\left(\frac{W_F(r_F)}{U}\right)_{tA} = \frac{ir_F N_A}{\pi^2\sqrt{1+a^2r_F^2}} \sum_{\substack{m=-\infty \\ m=\ell N_A}}^{\infty} e^{-i2m\Omega t}\, e^{im(\sigma_A+\sigma_F)}\, e^{-im\theta_{bF}\cos\varphi_\alpha}$$

$$\cdot \int_0^{\pi}\int_{\rho_A} e^{-im\theta_{bA}\cos\theta_\alpha} \sin\theta_\alpha \cos\theta_\alpha\, \rho_A \theta_{bA} \frac{t_o}{c}(\rho_A)\sqrt{1+a^2\rho^2_A}$$

$$\cdot \int_{-\infty}^{\infty} (IK)_m\, e^{i(\sigma_F-\sigma_A-a\epsilon)k/a}\left(ak - \frac{m}{r_F^2}\right) e^{-i\frac{k}{a}(\theta_{bF}\cos\varphi_\alpha - \theta_{bA}\cos\theta_\alpha)}\, dk d\rho_A d\theta_\alpha \tag{A-6}$$

The θ_α-integral involves

$$\int_0^{\pi} e^{i(k/a-m)\theta_{bA}\cos\theta_\alpha} \sin\theta_\alpha \cos\theta_\alpha\, d\theta_\alpha$$

$$= \int_0^{\pi} e^{i(u/a)\theta_{bA}\cos\theta_\alpha} \sin\theta_\alpha \cos\theta_\alpha\, d\theta_\alpha \quad \text{(letting } u=k-am\text{)}$$

$$= \frac{i2a^2}{\theta^2_{bA}} F(u,\rho_A) \tag{A-7}$$

where $F(u,\rho_A) = \left[\dfrac{\sin(u\theta_{bA}/a) - (u\theta_{bA}/a)\cos(u\theta_{bA}/a)}{u^2}\right]$

After substituting (A-7) and u=(k-am) in (A-6) and applying the generalized lift operator (see Eq. 7a), the velocity becomes, for each lift operator mode $\bar{m}$,

$$\left(\frac{\bar{W}_F^{(\bar{m})}(r_f)}{U}\right)_{tA} = -\frac{2a^2 r_F N_A}{\pi^2\sqrt{1+a^2r_F^2}} \sum_{\substack{m=-\infty \\ m=\ell N_A}}^{\infty} e^{-i2m\Omega t}\, e^{im(2\sigma_F - a\epsilon)}$$

$$\cdot \int_{\rho_a} \frac{\rho_A}{\theta_{bA}} \frac{t_o(\rho_A)}{c} \sqrt{1+a^2\rho_A^2}$$

$$\cdot \int_{-\infty}^{\infty} I_m(|u+am|\rho_A)\, K_m(|u+am|r_F)\, e^{i(\sigma_F-\sigma_A-a\epsilon)u/a} \left(au+a^2m-\frac{m}{r_F^2}\right)$$

$$\cdot\, I^{(\bar{m})}((-u-2am)\theta_{bF}/a)\, F(u,\rho_A)\, du\, d\rho_A \qquad \text{(A-8)}$$

for $\rho_A < r_F$, otherwise ρ_A and r_F are interchanged in the modified Bessel functions. On changing the doubly infinite u-integral to an integral from 0 to $+\infty$, (A-8) can be written as

$$\left(\frac{\bar{W}_F^{(\bar{m})}(r_F)}{U}\right)_{tA} = -\frac{2a^2 r_F N_A}{\pi^2\sqrt{1+a^2r_F^2}} \sum_{\substack{m=-\infty \\ m=\ell NA}}^{\infty} e^{i2m\Omega t}\, e^{-im(2\sigma_F - a\epsilon)}$$

$$\cdot \int_{\rho_A} \frac{\rho_A}{\theta_{bA}} \frac{t_o}{c}(\rho_A) \sqrt{1+a^2\rho_A^2} \int_0^{\infty} F(u,\rho_A)$$

$$\cdot \Big\{ I_m(|u-am|\rho_A)\, K_m(|u-am|r_F)\, e^{i(\sigma_F-\sigma_A-a\epsilon)u/a}$$

$$\cdot \left(au-a^2m+\frac{m}{r_F^2}\right) I^{(\bar{m})}((-u+2am)\theta_{bF}/a)$$

$$+ I_m(|u+am|\rho_A)\, K_m(|u+am|r_F)\, e^{-i(\sigma_F-\sigma_A-a\epsilon)u/a}$$

$$\cdot \left(au+a^2m-\frac{m}{r_F^2}\right) I^{(\bar{m})}((u+2am)\theta_{bF}/a) \Big\}\, du\, d\rho_A \qquad \text{(A-9)}$$

where the sign of m is also changed, which is permissible since the m series is doubly infinite. The integrand of (A-9) is zero when u=0 since

$$F(0,\rho_A) = \lim_{u\to o}\left[\frac{\sin(u\theta_{bA}/a) - (u\theta_{bA}/a)\cos(u\theta_{bA}/a)}{u^2}\right] = 0$$

In the steady-state condition, $m=\ell=0$, the velocity on the forward propeller due to the blade thickness of the after propeller, $\left(\frac{\bar{W}_F^{(o,\bar{m})}(r_F)}{U}\right)_{tA}$, can be shown to be as given in Eq. (13) of the text. The unsteady velocity components are at frequencies $2m\Omega = 2\ell N_A\Omega$, with $\ell = \pm1,\pm2,\ldots$, and are given by

$$\begin{aligned}\left(\frac{\bar{W}_F^{(m,\bar{m})}}{U}\right)_{tA} e^{i2m\Omega t} &= \left(\frac{\bar{W}_F^{(1\ell IN_A,\bar{m})}}{U}\right)_{tA} e^{i21\ell IN_A\Omega t} \\ &\quad + \left(\frac{\bar{W}_F^{(-1\ell IN_A,\bar{m})}}{U}\right)_{tA} e^{-i21\ell IN_A\Omega t} \\ &= \left[\left(\frac{\bar{W}_F^{(1\ell IN_A,\bar{m})}}{U}\right)_{tA} + conj\left(\frac{\bar{W}_P^{(-1\ell IN_A,\bar{m})}}{U}\right)_{tA}\right] e^{i21\ell IN_A\Omega t} \\ &= 2\left(\frac{\bar{W}_F^{(1\ell IN_A,\bar{m})}}{U}\right)_{tA} e^{i21\ell IN_A\Omega t} \qquad \text{(A-10)}\end{aligned}$$

Here $\left(\frac{\bar{W}_F^{(1\ell IN_A,\bar{m})}}{U}\right)_{tA}$ is the coefficient of $\exp(i2m\Omega t)$ in (A-9) with $m = 1\ell IN_A$ and is half the velocity at $21\ell IN_A$ times the shaft frequency. This velocity is designated as

$$\left(\frac{\bar{W}_F^{(2\ell N_A,\bar{m})}(r_F)}{U}\right)_{tA}$$

and is given by Eq. (14) of the text.

11. The velocity potential due to the blade thickness of the forward propeller at a point (x_A, r_A, φ_A) on the after propeller is given by (cf. (A-1) and (A-2))

$$\left(\Phi_A(x_A, r_A, \varphi_A; t)\right)_{tF} = -\frac{U}{2\pi} \sum_{n=1}^{N_F} \int_0^{\pi} \int_{\rho_F} \frac{\partial_F(\rho_F, \theta_\alpha)}{\partial \theta_\alpha} \frac{\sqrt{1+a^2\rho_F^2}}{R_{FA}} \, d\rho_F \, d\theta_\alpha \qquad (A\text{-}11)$$

where $R_{FA} = \left\{(x_A' - \xi_F)^2 + r_A^2 + \rho_F^2 - 2r_A\rho_F\cos\left[-\theta_{F0} - \varphi_{F0} + 2\Omega t + \bar{\theta}_{Fn}\right]\right\}^{1/2}$

$$x_A' = \varphi_{A0}/a + \epsilon = (\sigma_A - \theta_{bA}\cos\varphi_\alpha)/a + \epsilon$$

$$\xi_F = \theta_{F0}/a = (\sigma_F - \theta_{bF}\cos\theta_\alpha/a$$

and again approximating the thickness distribution by a lenticular section

$$\frac{\partial f}{\partial \theta_\alpha} \approx 2\frac{t_o}{c}(\rho_F) \cdot \rho_F \, \theta_{bF} \sin\theta_\alpha \cos\theta_\alpha$$

The velocity normal to the blades of the after propeller due to this velocity potential is

$$(W_A)_{tF} = -\frac{\partial}{\partial n_A'}(\Phi_A)_{tF} = -\frac{r_A}{\sqrt{1+a^2r_A^2}}\left(\frac{a\partial}{\partial x_A'} - \frac{1}{r_A^2}\frac{\partial}{\partial \varphi_{A0}}\right) \qquad (A\text{-}12)$$

If the procedure of the preceding section is followed, it can be easily shown that the velocity normal to the blades of the after propeller induced by the forward propeller thickness is in the steady-state given by Eq. (15) of the text and in the unsteady case at frequencies equal to $2l\ell N_F$ times the shaft frequency given by Eq. (16).